

Crossing Angle Collision and Lifetime: Simulations, Analysis, Measurements and More Simulations

Tong Chen[†]

Stanford Linear Accelerator Center, Stanford University, Stanford, CA94309

I. INTRODUCTION

In order to achieve the high luminosity required by heavy quark factories, multi-bunch operation is almost the only choice. The key to gain luminosity in multi-bunch operation is to reduce the bunch spacing. Therefore, colliding beams with a crossing angle becomes the favorite interaction region scheme.

The introduction of a crossing angle in e^+e^- colliders causes non-linear coupling between horizontal motion and longitudinal motion. This is illustrated in Figure 1. The beam-beam kick occurs when the particle passes the center of the opposing bunch. The strength of the kick, $\Delta r' = F(r)$, is a nonlinear function of the distance, r , between the particle and the center of the opposite bunch. In head-on collisions, r is the transverse displacement, and the kick is in the transverse plane, so that the process is nonlinear but not influenced by the longitudinal motion. In collisions with a crossing angle, however, r is a function of longitudinal displacement, s , and the crossing angle, Φ , as well as transverse displacement. The distance r between the test particle and the bunch center can be written as:

$$r = x + \tan \Phi \cdot s \tag{1}$$

[†] Work supported in part by the Department of Energy Contract DE-AC03-76SF00515

The kick is a function of both transverse and longitudinal positions and, as a result, non-linear synchro-betatron coupling is generated by the crossing angle collision.

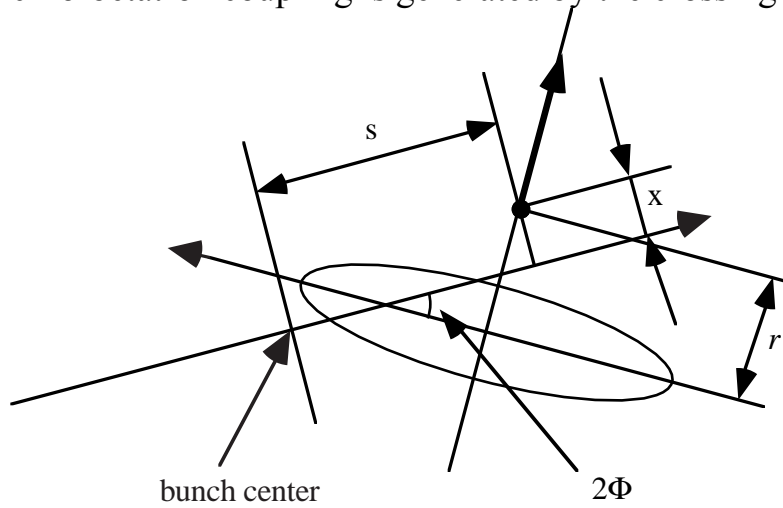


Figure 1. Kick in crossing angle collision

Previous experience on crossing angle collision indicate that the major problem is having bad lifetime. Following discussion will concentrate on this issue.

II. PRELIMINARY SIMULATIONS

A simple simulation program similar to Piwinski's work^[1] was written to study the crossing angle collision problem. The simulation program adopts a weak-strong beam-beam interaction model, and consists of only a single beam-beam kick and a linear map for the ring. The beam-beam kick incorporates the crossing angle collision. Three dimensional motion is simulated. Particles are launched in six dimensional phase space with 6σ amplitudes, which are the typical large amplitude particle that may affect lifetime. For convenience of studying resonances, the program scans the horizontal fractional tune from 0 to 1. The maximum amplitude of all particles ever reached during the 1000-turn tracking is recorded as a function of horizontal tune.

The simulation was performed based on CESR B design. The half crossing angle Φ is 10 mrad. The beam sizes σ_x and σ_s , are taken as 0.36mm and 1cm respectively. The normalized crossing angle, defined as $\frac{\sigma_s}{\sigma_x} \Phi$, is 0.278. The results of a simulation with $\Phi=10\text{mrad}$ crossing angle are shown in figure 2. Some one-dimensional resonances, such as $Q_x=1/2, 1/4$ and $1/6$, already exist in head-on collision. They are not introduced by the crossing angle. Besides these resonances, one can find many synchro-betatron resonances appeared. The strongest new resonances are identified as $5Q_x \pm Q_s = \text{integer}$ resonances. The coupling resonance $Q_x \pm Q_s = \text{integer}$ can also be seen in this picture.

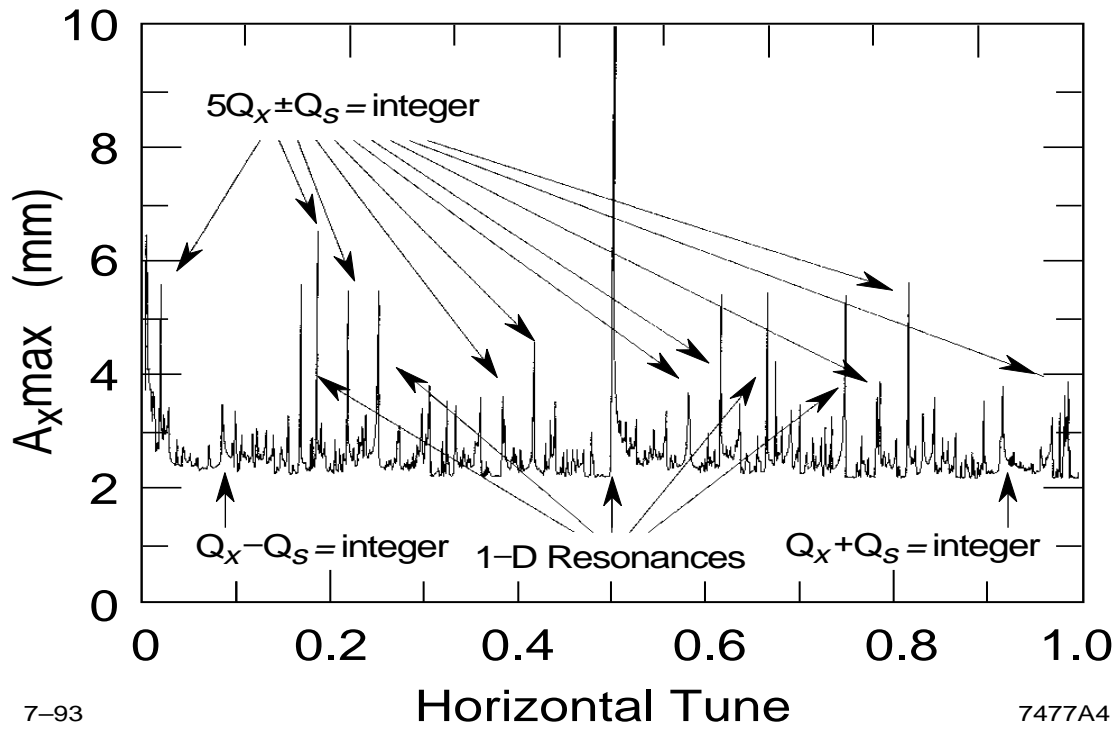


Figure 2. Maximum horizontal amplitude vs. tune for crossing angle collision.
($Q_s=0.081$)

III. ANALYSIS

From the simulation result of previous section, one would ask why the particular resonance family, $5Q_x \pm Q_s = \text{integer}$, is excited. To answer this question, a resonance analysis method is introduced here. The analysis is good for a linear storage ring with a single nonlinear thin element^[2], which is a reasonable approach to the beam-beam interaction problem. This method is developed to employ the Fourier Transform to expand the non-linear force, and relates the Fourier expansion components to certain resonances.

In the crossing angle problem, we are interested in the horizontal (x) and longitudinal (s) motion. Two dimensional difference equations are used to describe the motion. If we sit at one point of a linear ring observing a particle, its motion can be described by :

$$x_{t+1} - 2x_t \cos \mu_x + x_{t-1} = 0 \quad (2)$$

$$s_{t+1} - 2s_t \cos \mu_s + s_{t-1} = 0 \quad (3)$$

where t stands for turn number and μ_x and μ_s are the whole-turn phase advances of the oscillations. It is straight forward to find their solutions:

$$x_t = A_x \cos(\mu_x t) \quad (4)$$

$$s_t = A_s \cos(\mu_s t). \quad (5)$$

With the crossing angle collision, the difference equations become:

$$x_{t+1} - 2\cos \mu_x x_t + x_{t-1} = -\beta_x \sin \mu_x F(x_t + \tan \Phi \cdot s_t) \cos^2 \Phi \quad (6)$$

$$s_{t+1} - 2\cos \mu_s s_t + s_{t-1} = \beta_s \sin \mu_s F(x_t + \tan \Phi \cdot s_t) \sin \Phi \cos \Phi. \quad (7)$$

where F is the horizontal beam-beam kick, which can be approximated by a Dawson's integral^[3]:

$$F(r) = F_d\left(\frac{r}{\sqrt{2}\sigma_x}\right) \quad (8)$$

$$\text{and } F_d(y) = e^{-y^2} \int_0^y e^{t^2} dt. \quad (9)$$

where σ_x is the horizontal beam size. β_s can be defined in an analogous way to the transverse motion^[4]. In the difference equations (6) and (7), the kick modulation of the arrival time is neglected. This is because: (1), The β_x at the IP is much larger than the bunch length. The β_x change in the bunch length range is negligible. (2), If the kick ($\Delta x'$) is transferred back to the IP through drift space, it has the same amount. For small crossing angle Φ , the non-linear kick in the longitudinal plane is very weak. In addition, the longitudinal emittance is much larger than the horizontal emittance, which means s is much larger than x . Therefore, the longitudinal non-linear kick is negligible. Thus, the above equations are simplified:

$$x_{t+1} - 2\cos\mu_x x_t + x_{t-1} = -\beta_x \sin\mu_x F(x_t + \tan\Phi \cdot s_t) \cos^2\Phi \quad (10)$$

$$s_{t+1} - 2\cos\mu_s s_t + s_{t-1} = 0. \quad (11)$$

Equation (11) has the same solution as (5). As the first step approximation, substitute (4) into the right hand side of (10). Particles at large amplitude were used to evaluate the resonances, because previous studies have shown that crossing angles would mostly affect the large-amplitude particles^[1]. 6σ amplitude is chosen because it is the typical amplitude for large amplitude particles which we concentrate on, and changes near this amplitude does not change the qualitative conclusion. Taking $A_x = 6\sigma_x$ and $A_s = 6\sigma_s$, the Dawson's integral becomes:

$$F_d\left(\frac{6}{\sqrt{2}} \frac{\sigma_x \cos\mu_x t + \sigma_s \tan\Phi \cos\mu_s t}{\sigma_x}\right). \quad (12)$$

From (12), we notice that the coupling term is actually proportional to $\frac{A_s}{\sigma_x} \tan\Phi$, rather than $\tan\Phi$. Since $A_s \sim \sigma_s$, the coupling generally scales as $\frac{\sigma_s}{\sigma_x} \tan\Phi$. This is called the normalized crossing angle.

Expanding the non-linear kick in a two-dimensional Fourier Series, the right hand side of (10) can be written as:

$$\text{RHS} = \frac{1}{2} \sum_{m,n} c_{m,n} \cos[(m\mu_x + n\mu_s)t] + d_{m,n} \cos[(m\mu_x - n\mu_s)t] \quad (13)$$

Similarly, a solution is expected in the form:

$$x_t = \frac{1}{2} \sum_{m,n} a_{m,n} \cos[(m\mu_x + n\mu_s)t] + b_{m,n} \cos[(m\mu_x - n\mu_s)t] \quad (14)$$

Substituting the above equations into (10), it is easy to find the resonance driving relations:

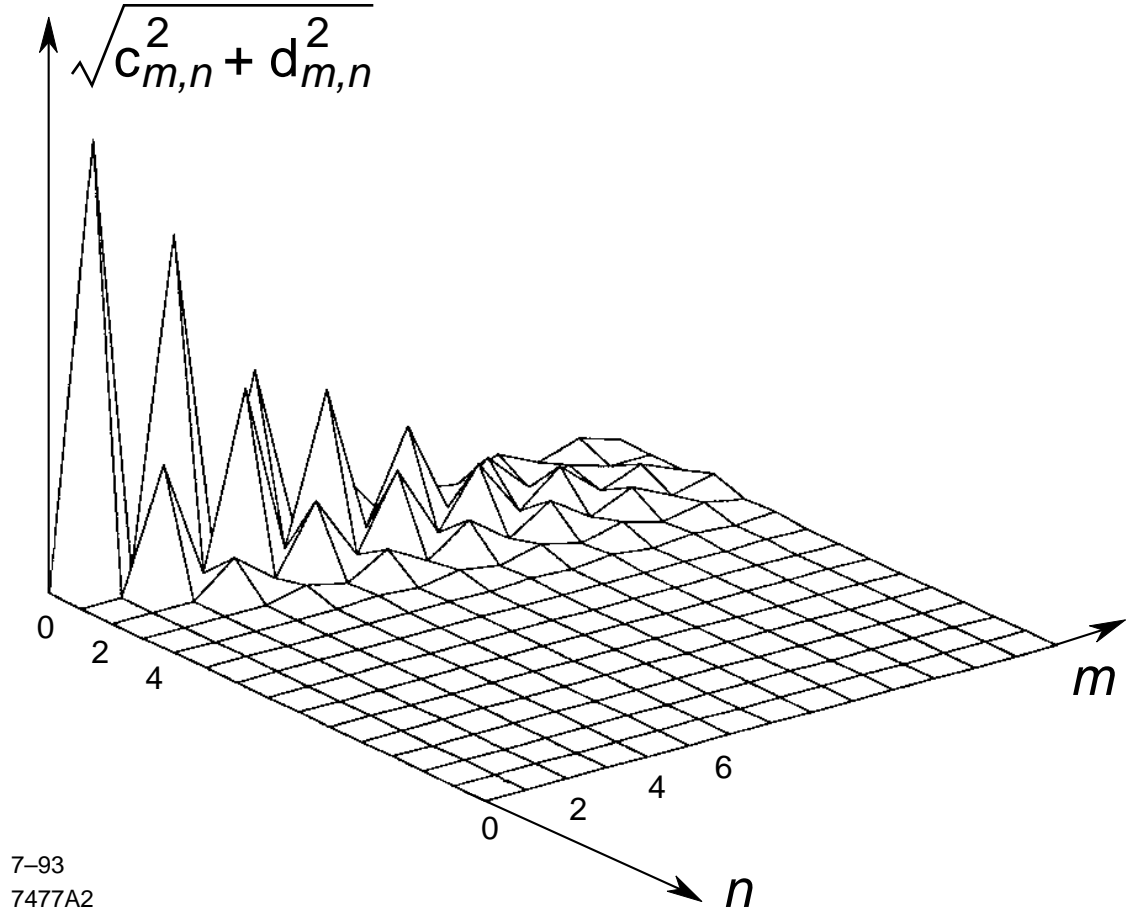
$$a_{m,n} = \frac{c_{m,n}}{2\sin\frac{1}{2}[(m+1)\mu_x + n\mu_s]\sin\frac{1}{2}[(m-1)\mu_x + n\mu_s]} \quad (15)$$

$$b_{m,n} = \frac{d_{m,n}}{2\sin\frac{1}{2}[(m+1)\mu_x - n\mu_s]\sin\frac{1}{2}[(m-1)\mu_x - n\mu_s]}. \quad (16)$$

Near resonances $(m \pm 1)Q_x \pm nQ_s = \text{integer}$, the denominator is small. Then, $(a,b)_{m,n}$ has strong response to $(c,d)_{m,n}$. Therefore, we can say that $c_{m,n}$ and $d_{m,n}$ drive these resonances.

Figure 3 shows the power spectrum of the Dawson's integral (12), created by two-dimensional FFT. The power spectrum $\sqrt{c_{m,n}^2 + d_{m,n}^2}$ gives the resonance driving strength. The phase of the driving terms are not important. Due to the symmetry

of the function, the terms with $m+n=\text{even}$ vanish. In the calculation, the parameter are the same as the simulation.



7-93
7477A2

Figure 3. The power spectrum of the crossing angle beam-beam kick.

From figure 3, we can easily see that, besides the 1-dimensional resonance driving terms($n=0$), the strongest coupling resonance ($n \neq 0$) driving terms are those with $m=4, n=1$ and $m=6, n=1$. According to the previous analysis, these two terms will drive $3Q_x \pm Q_s = \text{integer}$, $5Q_x \pm Q_s = \text{integer}$ and $5Q_x \pm Q_s = \text{integer}$, $7Q_x \pm Q_s = \text{integer}$ resonances respectively. It is natural to conclude that the $5Q_x \pm Q_s = \text{integer}$ resonances are the strongest coupling resonances, since they are driven by both of the two largest driving terms. This conclusion consists with the simulation result. Note that the spectrum in Figure 3 is a function of the

normalized crossing angle. The conclusion here is only for the small normalized crossing angle.

IV. MEASUREMENTS

The experiment is designed to observe the $5Q_x + Q_s$ resonance associated with crossing angle collision, which is predicted by the theory in previous section and simulations. The theory shows that the $5Q_x \pm Q_s$ resonances are driven for large amplitude particles, and simulation shows these particles are sent to even larger amplitudes, which can result in losing those particles. Therefore, one should expect to see a bad lifetime near those resonances.

The experiment is based on the setup of the CESR crossing angle experiment^[5]. CESR has been running with multi-bunch mode (7 bunches of e^- on 7 bunches of e^+). The key point of making multi-bunch mode possible is to separate bunches around the ring except at the interaction point where the detector is located. In CESR, four electrostatic separators were used to separate electron and positron orbits at parasitic crossing points. As shown in figure 4, the orbits (thin lines) were separated at 13 would-be collision points, but were merged between the two south (lower) separators, including the interaction point (IP) where the collision takes place. The crossing-angle lattice is essentially a modified version of the normal-operation lattice. The experiment was performed with one bunch on one bunch. A certain amount of anti-symmetric voltage was applied to the south separators, which creates anti-symmetric orbits about the IP. This is displayed in figure 5 as the thick lines. It is easy to see from the picture that the beams will collide at the IP with an angle. The half crossing angle can go up to about ± 2.5 mrad. The crossing angle is limited by the physical aperture at the interaction region (IR) quadrupoles, where the closed orbit is moved to 8.6σ from vacuum chamber.

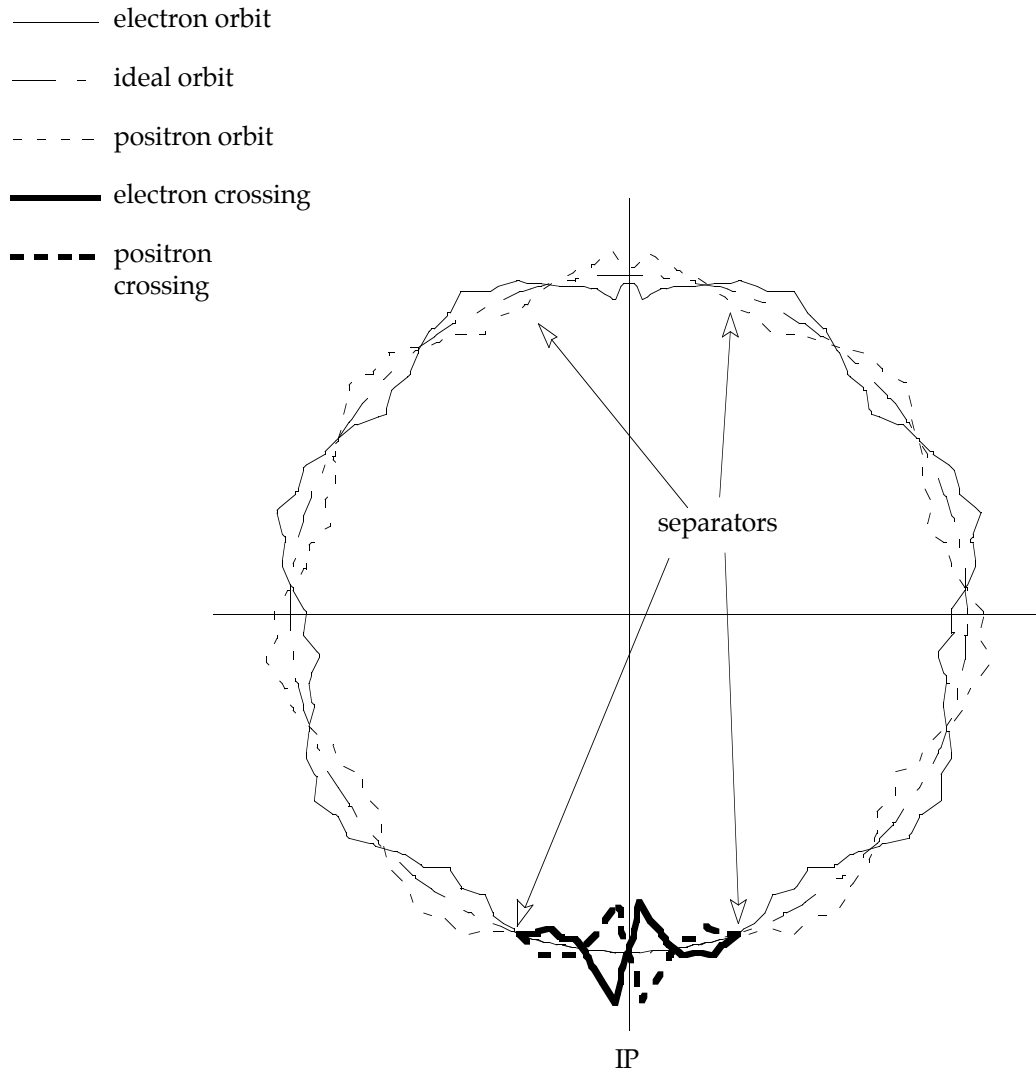


Figure 4. Diagram of the orbits for the crossing angle experiment

The procedure of the experiment is similar to the simulation: scan the horizontal tune while the beams collide at an angle, and measure the decay rate (time derivative of the beam current). The weak-strong scenario is reproduced via collisions of a 2 mA beam of electrons and a 10 mA beam of positrons. The tune scan is carried out near the $5Q_x + Q_s = 43$ (for $Q_s=0.064$, $Q_x=8.587$) resonance. The reason to choose this resonance is that the crossing angle lattice working point is close to the resonance (nominal horizontal tune $Q_x=8.57$). It is easy to move the

tune to the vicinity of the resonance. In addition, simulation shows that this resonance is in a “clean” area, *i.e.*, there are no other strong resonances near by.

The experiment consists two measurements. The first one is to measure $5Q_x+Q_s$ resonance with and without crossing angle. The synchrotron tune was $Q_s = 0.0628$.

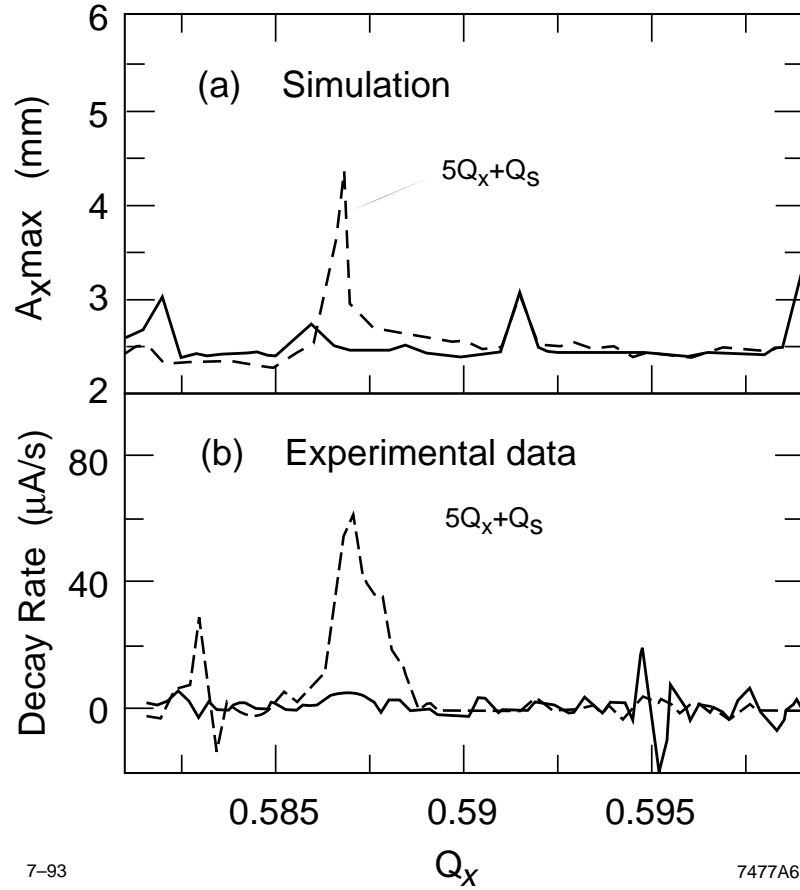


Figure 5. (a). Simulation result, maximum amplitude versus horizontal tune. (b). Experimental data, decay rate as a function of horizontal tune. Solid lines are the head-on collision data, and dashed lines are the crossing angle data.

For comparison, figure 5 gives both the simulation and experimental results. Figure 5a shows the simulation results for head-on collisions (solid line) and crossing angle collisions (dashed line). The plot gives the maximum horizontal

amplitude as a function of horizontal tune. It shows that the $5Q_x+Q_s$ resonance appears only when the beams collide at an angle. Figure 5b plots the measured results. The data is from two separate measurements: one with the crossing angle turned on (dashed line), and the other one with the angle turned off (solid line). Both measurements employ strong-weak collisions, *i. e.*, 10 mA positron on 2 mA electron. The weak beam (electron) is driven by the resonance, suffering bad lifetime (or large decay rate). The decay rate is obtained by digitally differentiating the electron current versus time (as the result of differentiation, some jitters in the current measurement creates bi-polar spikes, which result in unrealistic negative decay rates). The predicted resonance at $Q_x=0.587$ appears in the data plotted in figure 5.

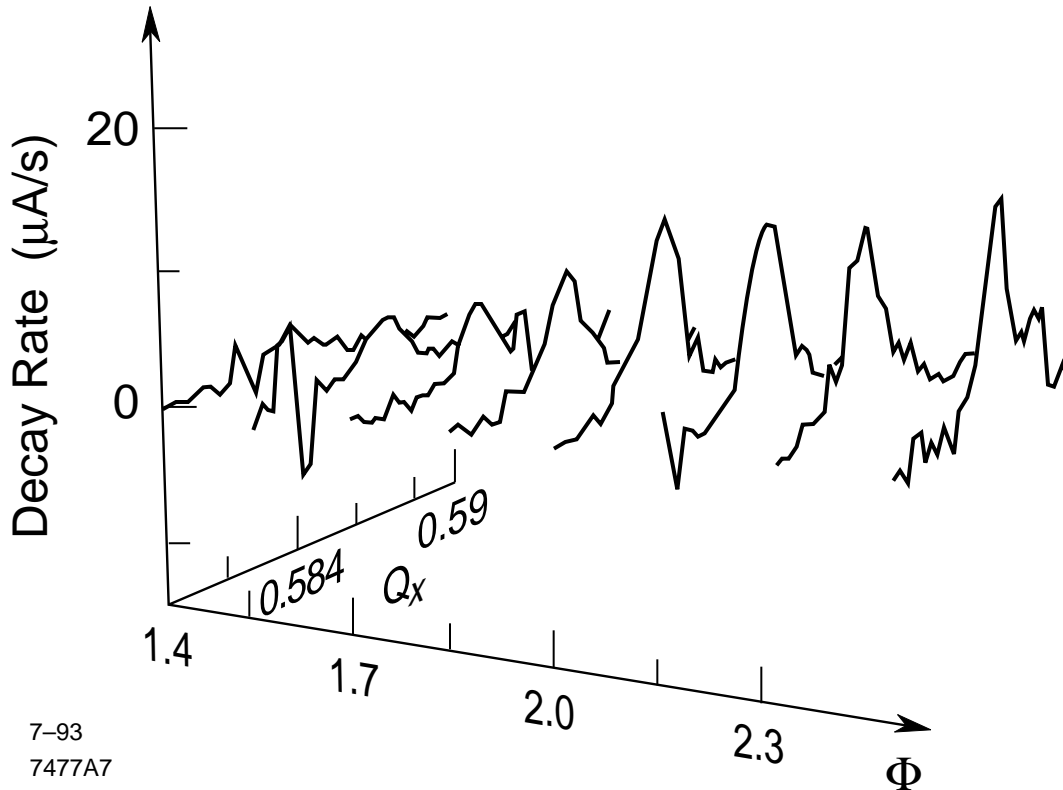


Figure 6. Tune scans versus different crossing angles.

The second measurement is the resonance ($5Q_x+Q_s$) strength as a function of crossing angle. The crossing angle was set to different values and a one-

dimensional tune scan was performed to measure the decay rate as a function of tune at each angle. The angle is controlled by the anti-symmetric voltage applied to the south separators. Figure 6 gives the measured results. Test runs have indicated that the resonance is not measurable for half crossing angle smaller than 1.4 mrad. Hence, detailed measurements took place at larger half crossing angles, up to 2.4 mrad. The picture shows a clear ridge of the decay rate at the $5Q_x+Q_s$ resonance, growing as the crossing angle increases.

V. LIFETIME SIMULATIONS

The simulation described in section II tracks only 1000 particles for 1000 turns, which is far not enough to provide lifetime information. To simulate the lifetime, extremely long CPU time is required. A new technique was proposed by J. Irwin to do the simulation with dramatically reduced CPU time^[6]. With this method, we can investigate the development of beam-beam tails and calculate lifetime^[7].

Using the new program, the simulation is repeated. Similar to the experiments, tune scan and angle scan are simulated separately. The simulation gives the lifetime as a function of horizontal and vertical apertures. In the crossing angle case, horizontal tail excited by the $5Q_x+Q_s$ resonance dominates the lifetime. Figure 7 plotted the simulated lifetime at the horizontal aperture of 8.5σ . The measurement data, converted from that of figure 5 (b), is shown in the same plot.

The angle scan simulation was done at $Q_x=0.5855$. The half crossing angle was scanned from 1.2 mrad to 2.4 mrad. The lifetime at $8.5 \sigma_x$ is shown in figure 8. The minimum lifetime at various angles from the data in figure 6 is also plotted for comparison.

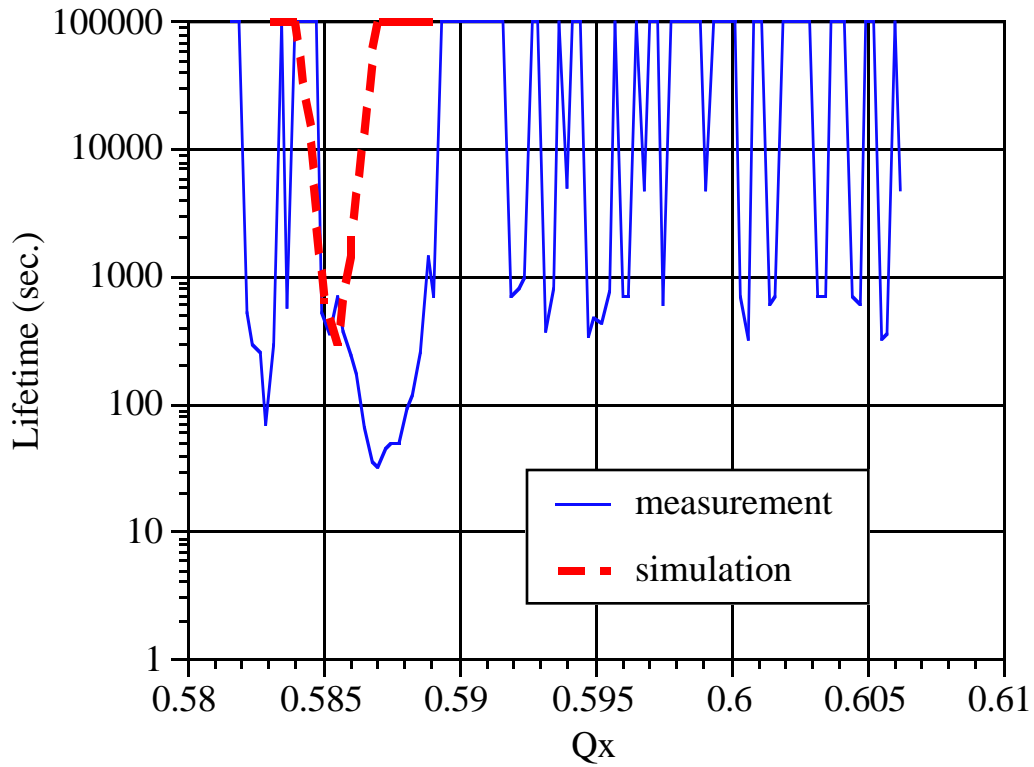


Figure 7. The lifetime versus tune near $5Q_x + Q_s$ resonance. Simulation and measurement results are compared.

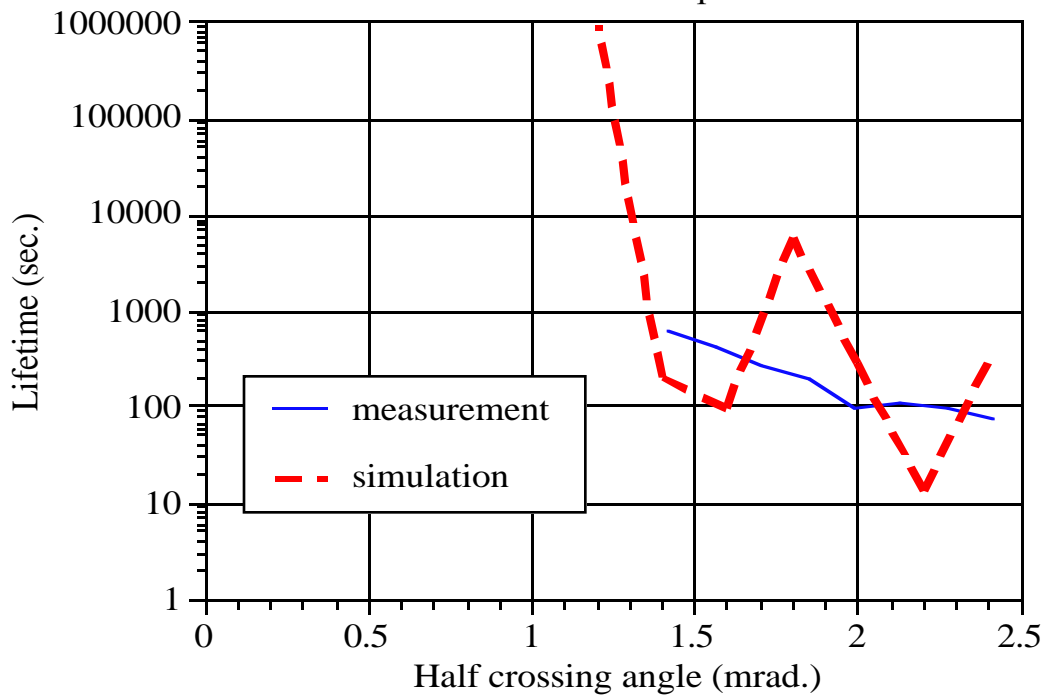


Figure 8. Lifetime versus half crossing angle. Simulation and measurement.

VI. REMARKS

This is one of the preliminary attempt to compare simulated lifetime with measurements. In the tune scan data, the minimum lifetime at the resonance is missing by a factor of 10. For the angle scan data, simulated results fluctuate strongly.

Many uncertainties may affect the simulation results. The aperture that determines the lifetime is not well known, and it is a sensitive parameter. The most important factor, I believe, is the lattice errors. Studies have shown that lattice errors, including nonlinearities, solenoid coupling, misalignment, chromaticities, etc., can dramatically change the tail distribution, as well as lifetime. For CESR, these are not negligible. However, there is not enough information on those errors to put in the simulation.

VII. ACKNOWLEDGMENT

Author would like to thank M. Tigner, D. Rubin, D. Rice, D. Sagan and CESR operating group who involved in the crossing angle studies, especially making measurements on CESR. Author also want to thank R. H. Siemann and J. Irwin for working together on the beam-beam lifetime simulations.

VIII. REFERENCES

- [1] Piwinski, A., "Simulations of Crab Crossing in Storage Rings," SLAC-PUB-5430, Feb. 1991.
- [2] Peggs, S. and Talman, R., "Nonlinear Problems in Accelerator Physics," *Ann. Rev. Nucl. Part. Sci.* , vol. 36, 287, 1986.
- [3] Peggs, S., Ph. D. Thesis, Cornell University 1981
- [4] Chen T., Ph. D. Thesis, Cornell University, January 1993

- [5] Rubin, D. and *et al*, “Beam-beam Interaction with a Horizontal Crossing Angle,” *Nuclear Instruments and Methods in Physics Research A330*, p12, (1993) / CLNS 92/1183.
- [6] J. Irwin, Proc. of the 3rd Advanced ICFA Beam Dynamics Workshop, Novosibirsk, USSR, 123 (1989) /SLAC-PUB-5743, Feb. 1992.
- [7] T. Chen, J. Irwin and R. Siemann, Physical Review E, Vol. 49, No. 3, p2323, March 1994.